Atatürk Üniversitesi
Anadolu Fizik ve Astronomi Dergisi
(ISSN: 2791-8718)
Cilt 2, Sayı 1,1-17

Atatürk University
Journal of Anatolian Physics and Astronomy
(ISSN: 2791-8718)
Volume 2, Issue 1,1-17

JAPA

Synthesis of Reduced Graphene Oxide (rGO) Supported Pt Nanoparticles via Supercritical Carbon Dioxide Deposition Technique for PEM Fuel Cell Electrodes

*[1,2] Elif DAŞ and [2,3] Ayşe BAYRAKÇEKEN YURTCAN

[1]Department of Physics, Faculty of Science, Atatürk University, Erzurum, 25240, Turkey
[2]Department of Nanoscience and Nanoengineering, Graduate School of Natural and Applied Science, Atatürk University, Erzurum 25240, Turkey
[3]Department of Chemical Engineering, Faculty of Engineering, Atatürk University, Erzurum 25240, Turkey

ORCID*[1]:https://orcid.org/0000-0002-3149-6016

Research Type: Research Article
Received: 15.03.2022, Accepted: 03.04.2022
*Corresponding author: das.elif@gmail.com (E.Daş)

Abstract

In this work, the preparation of reduced graphene oxide (rGO) supported Pt nanoparticles by using the supercritical carbon dioxide ($scCO_2$) deposition technique is investigated. For this purpose, firstly, graphite oxide synthesis was made similar to the literature reports and then two different reducing agents (DMF and hydrazine hydrate) were used to prepare rGO support materials, called as rGO1 and rGO2, respectively. Finally, Pt nanoparticles (NPs) were formed on the rGO support materials. The effect of the reducing agent type and also of the catalyst preparation technique on the fuel cell performance were examined with spectroscopic, microscopic, and electrochemical techniques. From the results obtained, it appears that the properties of rGO vary significantly depending on the reducing agent used. Moreover, the electrode containing Pt/rGO1 has exhibited better cell performance compared to the Pt/rGO2.
Key Words: PEM fuel cell electrodes, Pt nanoparticles, support material, reducing agent.

PEM Yakıt Pili Elektrotları için Süperkritik Karbondioksit Depozisyon Tekniği ile İndirgenmiş Grafen Oksit (rGO) Destekli Pt Nanoparçacıklarının Sentezi

Özet

Bu çalışmada, süperkritik karbondioksit depozisyon tekniği ($scCO_2$) kullanılarak indirgenmiş grafen oksit destekli (rGO) Pt nanoparçacıklarının sentezi araştırılmaktadır. Bu amaçla, öncelikle, literatüre benzer olarak grafit oksit sentezi gerçekleştirildi ve daha sonra iki farklı indirgeyici ajan (DMF ve hidrazin hidrat) ile sırasıyla rGO1 ve rGO2 olarak isimlendirilen rGO destek malzemeleri hazırlandı. Son olarakta, Pt nanoparçacıkları (NPs) rGO destek malzemeleri üzerine oluşturuldu. Indirgeyici ajan türünün ve katalizör hazırlama tekniğinin yakıt pili performansı üzerindeki etkisi spektroskopik, mikroskopik ve elektrokimyasal tekniklerle incelendi. Elde edilen sonuçlardan, kullanılan indirgeyici ajana bağlı olarak rGO malzemesinin özelliklerinin önemli ölçüde değiştiği görülmektedir. Ayrıca, Pt/rGO1 içeren elektrot, Pt/rGO2'ye kıyasla daha iyi pil performansı sergilemiştir.

Anahtar Kelimeler: PEM yakıt pili elektrotları, Pt nanoparçacıkları, destek malzemesi, indirgeyici ajan.

1. Introduction

Fuel cells are one of the important clean energy converting devices. Polymer electrolyte membrane fuel cells (PEMFCs) are the most studied among all types of fuel cells, especially for stationary, portable and automotive applications. It is mainly because of their high energy conversion efficiency, high energy density, low operation temperature, fast start-up and response times and low emission [1-4]. However, there are some critical obstacles preventing the commercialization and common usage of PEM fuel cells, such as high cost of platinum (Pt) catalysts and low durability of the catalyst layer [5-9]. For this reason, many strategies have been developed to increase catalytic activity and to reduce the usage of Pt-based catalysts. One of these strategies is to use carbon-based material as catalyst support [10-13]. Because support material not only provides conductivity but also provides a high surface area to improve the Pt utilization efficiency. Up to now, many alternative carbon-based materials such as carbon nanotubes, carbon aerogels, mesoporous carbon, fullerene, graphitic and carbon fibers have been tried as support materials [3, 14-20]. But, none of these prevalently used support materials can exactly fulfill the essential requirements. Hence, efforts must be put in for the development of new catalyst support.

In the past several years, graphene, with unrivalled 2D structure and properties including high conductivity, high specific surface area, high tensile strength, and etc., has been regarded as an alternative catalyst support for Pt nanoparticles (NPs) due to these superior features, have been commonly studied [21-26]. In literature, numerous methods have been developed to prepare graphene, including mechanical exfoliation of graphite (scotch-tape method), epitaxial growth, chemical vapor deposition, liquid phase exfoliation of graphite, chemical reduction of GO [27, 28]. Among all these methods, the chemical reduction of GO is the most promising method for mass production of graphene and this method involves of oxidation/reduction steps [29, 30]. Typically, graphite material is converted to GO via strongly oxidizing agents such as HNO_3, H_2SO_4, H_3PO_4, $KMnO_4$ and this oxidation step results in the widening of intersheet spacing of carbon layers due to the emplacement of functional groups onto the layer [31]. Following oxidation step, GO becomes hydrophilic in nature due to the polar oxygen functional groups and as a result, GO is easily dispersible in various solvents, especially in water [30]. The Van der Waals forces weaken because oxygen groups are

introduced in GO structure which results in a partial degradation of the sp^2 lattice into a sp^2-sp^3 sheet with less π-π stacking ability. These changes make GO non-conductive as it lacks the conducting graphitic network. The conducting property of GO can be recovered by the reduction process, such as chemical reduction (e.g. via reducing agents) and thermal reduction (e.g. via annealing at high temperature under inert gas), which eliminates functional groups. The efficiency of the reduction process can be measured with O/C ratio and this ratio decreases significantly after reduction process. Also, according to the literature reports, in the high electrical conductivity required applications, it is necessary to reduce the O/C ratio below 1% [2]. However, in some cases, partially reduction also is desired, because the surface functional groups on the material serve as the anchoring sides for metal NPs while preventing restacking and aggregation to graphite form during the chemical reduction to graphene. Therefore, many studies are conducted in the literature on the preparation of Pt NPs onto the graphene-based materials such as graphene nanoplatelets (GNPs), graphene nanosheets, rGO, and functionalized graphene (g-GO) [2, 24, 32-34].

Along with the catalyst support material used, the catalyst preparation technique is also momentous and among the proposed catalyst preparation techniques in the literature, $scCO_2$ deposition technique has attracted attention in last years, due to its important advantages [8, 35-37]. This technique employs the dissolution of a metal precursor in the $scCO_2$ environment leading to the adsorption of the precursor into the support. Later, the metal precursor is converted to the corresponding metal via ex-situ or in-situ ways [38]. Thereby, supported metal NPs are obtained.

In most of the earlier reports on the Pt/rGO catalysts, on one hand, Pt NPs were formed on support during the reduction process of graphite oxide (GO), on the other hand, common techniques were used to create Pt NPs on the support. In our work, firstly, production of rGO support materials were achieved by using two different reducing agents and then Pt NPs were employed over these supports materials by using $scCO_2$ deposition technique. As far as we know, the decoration of Pt NPs on rGO support materials with the help of this technique and their fuel cell performances is presented in the literature for the first time. So, we believe that our study will make important contributions to the literature.

2. Material and Methods

2.1. Materials

STREM brand 1,5-dimethyl platinum cyclooctadiene ($PtCODMe_2$) was purchased for using as Pt organometallic precursor. Natural graphite flakes (average particle size 325 mesh) were procured from Alfa Aesar and used as recieved. Potassium peroxodisulfate ($K_2S_2O_8$ ≥99.9%), phosphorous pentoxide (P_2O_5, ≥98%), sulfuric acid (H_2SO_4 98%), sodium nitrate ($NaNO_3$ ≥99.9%), potassium permanganate ($KMnO_4$ ≥99.9%), hydrogen peroxide (H_2O_2, 30%) were purchased from Sigma–Aldrich for use in GO synthesis and same brand dimethylformamide (DMF) and hydrazine hydrate were used as GO reducing agents. All chemicals were used without any further treatment. Also, high purity CO_2, N_2, O_2, H_2 gases were purchased from Habaş.

2.2. Preparation of Graphite Oxide (GO), Reduced Graphene Oxide (rGO) Materials

Firstly, GO synthesis was made from natural graphite powder by using improved synthesis proposed by Kovtyukhova et al. [39]. Subsequently, the GO was reduced with two different reducing agents (DMF and hydrazine hydrate) to obtain rGO materials. The details of the rGO synthesis procedure via DMF is descibed in our earlier report [40] and the resulting product was called as rGO1 in this study.

On the other hand, hydrazine hydrate material was also used as a reducing agent to the synthesis of rGO. Briefly, 0.5 g of dried GO was thoroughly dissolved in 0.5 L of water with the help of an ultrasonic bath until there was no visible particle in the solution. Subsequently, 5 mL of reducing agent was added into the solution and the reflux system was connected for the reduction process. The solution refluxed for 18 h at 100 ºC. When the reflux process was completed, floating black particles were observed on the solution, which is due to the reduction of GO. Lastly, the solution was cooled down to room temperature, filtered and washed several times with water and methanol, respectively. After evaporation of the solvents with the rotary evaporator, the final product was obtained was called as rGO2.

2.3. Synthesis of rGO Supported Pt NPs

Pt NPs were created on the rGO support materials by using $scCO_2$ deposition method in a high pressure vessel. The details of synthesis procedure were mentioned in our previous studies [37, 41, 42]. To eliminate similarity, the schematic view of the experimental setup was shown in Fig. 1.

2.4. Characterization of the Materials

2.4.1. Characterization of physical properties

The surface structure parameters of the support materials were analyzed with BET isotherms by using the Micromeritics 3Flex analyzer. The samples were degassed at 90 ˚C for 12 h before taking measurements. Thermogravimetric (TG) analysis was performed using a Netzsch thermal analyzer with the heating rate of 10 ºC/min and the flow rate of 30 mL/min in aluminum crucibles under air atmosphere. The Raman spectra of the pristine graphite, rGO1 and rGO2 materials were measured by using a WITech alpha 300R Raman system. Surface morphology and chemical composition of the support materials were observed by Zeiss Sigma 300 model scanning electron microscope (SEM), which is equipped with energy-dispersive X-ray spectroscopy (EDS). The homogeneity of the Pt NPs on the support materials were analyzed through the JEOL 2100 JEM transmission electron microscopy (TEM). TEM samples were prepared by dispersing supports and catalyst materials in ethanol to form a homogeneous suspension. Then, the suspension was dropped on copper grid for observation.

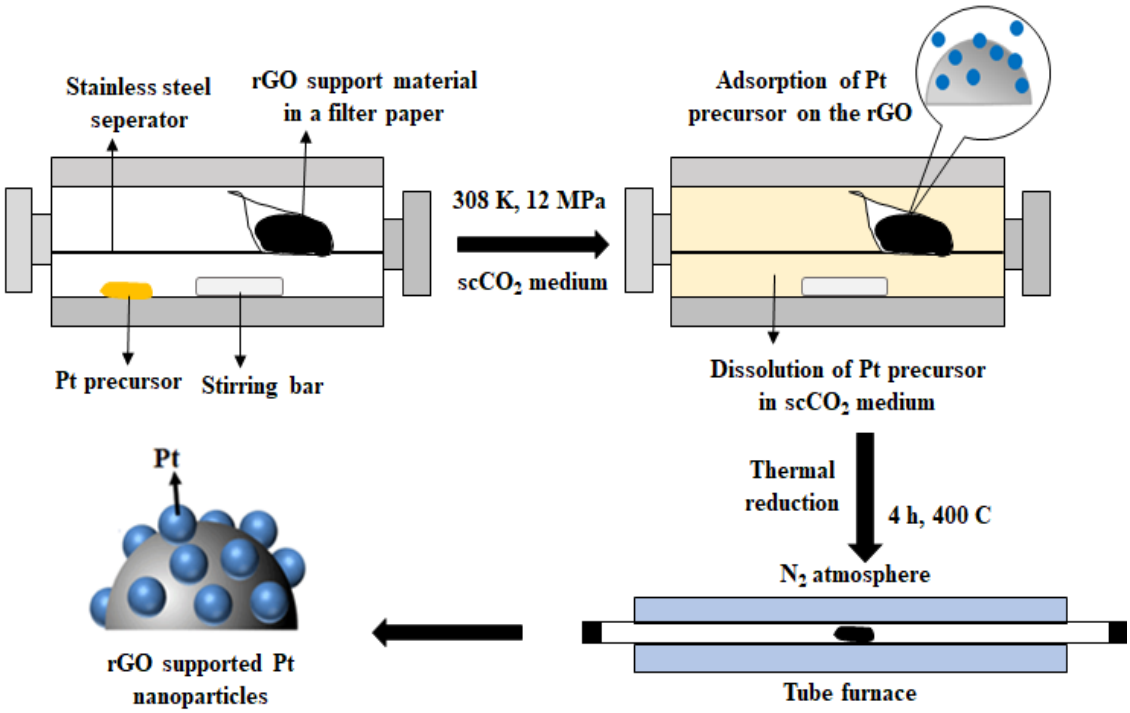

Figure 1. Experimental setup used for the decoration of Pt NPs on rGO support materials

2.4.2. Characterization of electrochemical properties

The ex-situ electrochemical studies of the support materials were performed in a standard three-electrode cell, using a VersaStat potentiostat/galvanostat. A silver-silver chloride electrode (Ag/AgCl, Cl^-) with 3.5 M KCI solution as a reference electrode, a Pt wire as a counter electrode and glass carbon (GC) as working electrode were employed. The obtained cycling voltammograms were converted and presented in terms of normal hydrogen electrode (NHE). To prepare working electrode catalyst ink, the required amount of the support material, deionized water, 1,2-propanediol and 15% Nafion solution were mixed till obtaining uniform ink. Then, the ink was dropped on the GC with a micropipette and left to dry at the room environment. The amount of the material on the GC was maintained as 22 μg/cm^2 for each electrode.

Cyclic voltammetry (CV) measurements for hydrogen oxidation reactions (HOR) were carried out in a N_2 saturated 1 M H_2SO_4 electrolyte (potential range: 0-1.2V, scan rate: 50 mV/s). Then, in order to apply electrochemical oxidation, the electrode was subjected to a constant potential of 1.2 V for 24 h. At the end of 24 h, the same test procedure was repeated. Thus, the oxidation characteristics of the rGO1 and rGO2 materials were evaluated before and after the electrochemical oxidation treatment. The tests were repeated several times for both support materials until the same results were obtained.

2.5. Fabrication of Membrane Electrode Assembly (MEA) and Fuel Cell Tests

The in-situ electrochemical tests were performed in a single fuel cell system (Henatech™). Firstly, cathode and anode electrodes were prepared. The details related to electrode preparation by using the spraying method can be found in our previous papers [4, 9]. The Pt loading was set to 0.4 mgPt/cm^2 for all catalyst layers. Then, prepared electrodes were hot pressed at 130 ºC and 400 psi for 3 min on to the Nafion 212 membrane to obtain MEA which has 4.41 cm^2 active surface area. Finally, the catalytic activities of MEAs were tested in a commercial PEM fuel cell test station. Hydrogen gas was fed from the anode side and oxygen gas fed from the cathode side, respectively. However, before the delivery of hydrogen and oxygen to the system, the cell was purged with nitrogen gas for a while. Meanwhile, the temperature of the cell and humidifier columns were adjusted to 70 °C. Subsequent to the purging, reactant gases were sent to the system. Then, polarization curves were taken by sweeping the voltage between OCV and 0.1V. In these measurements, the cell was equilibrated for at least 1 min at each point.

3. Results and Discussion

In heterogeneous catalysts, the vast majority of reactions take place on the catalyst surface. Therefore, it is very essential to accurately determine the surface area of the catalyst support. Likewise, the porosity and surface area knowledge of different support materials are of great importance in understanding their structure, formation, and potential applications. Surface area measurements are mainly carried out by the method of Brunauer, Emmett, and Teller (BET) [43]. According to this method, when a solid surface is reacted with a gas, the gas molecules attach to the surface and form adsorbed layers. The amount of adsorption is proportional to the total surface area of the sample. To determine the textural and structural properties of prepared support materials (rGO1 and rGO2), BET analysis was performed. The detailed BET results of rGO1 support material were given in our previous paper [40]. Hence, Fig. 2 shows the N_2 adsorption/desorption isotherms of the rGO2 support material and the corresponding pore size distribution. The isotherm of the rGO2 support material can be identified as type IV according to the International Union of Pure and Applied Chemistry (IUPAC) classification. Type IV isotherms are characteristic of materials containing mesopores and it shows a hysteresis loop from P/P_o=0.5 to P/P_o=1.0 which is H3 type hysteresis according to the IUPAC classification. This is attributed to the characteristic of aggregates of plate-like particles giving rise to slit-shaped pores and is common for carbon-like samples [44, 45].

According to the obtained BET results (Table 1), the surface area of the pristine graphite with a layered structure was found to be 13.7 m^2/g [40]. After the chemical oxidation process, it was observed that the material structure changed and a decrease in the surface area (3.3 m^2/g) occurred. Furthermore, after the reduction of GO with two different reducing agents, it was observed that the surface area values and pore volume values increased. However, the obtained surface area values were lower than the theoretical value (2630 m^2/g) of single graphene sheet. This is attributed to the restacking phenomenon of the graphene sheets owing to strong van der Waals forces.

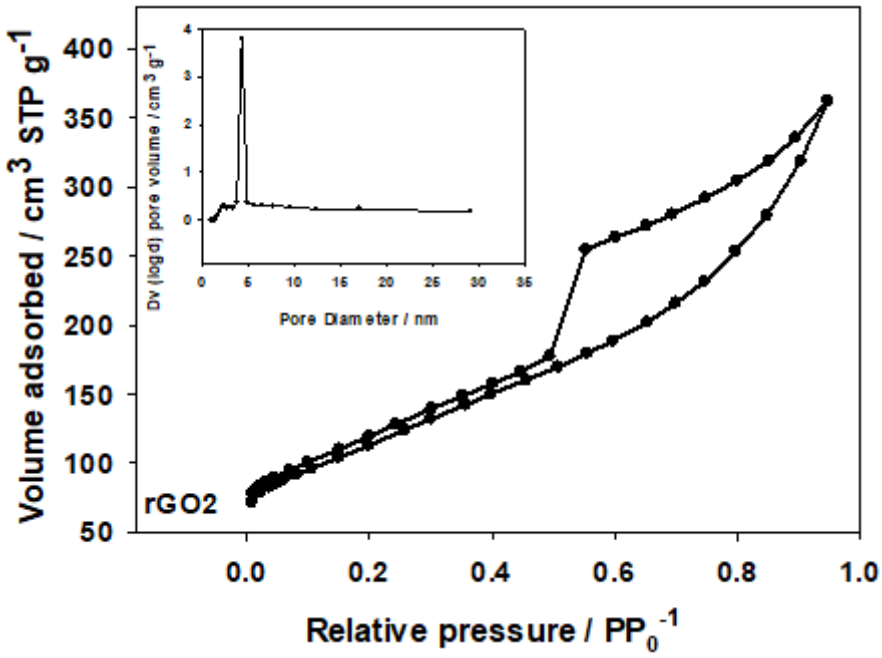

Figure 2. BET-N_2 adsorption/desorption isotherm and pore size distribution of the rGO2 support material

Table 1. Surface areas, pore volumes and pore sizes of the materials

Support	Total Surface Area (m^2/g)	BJH Pore Volume (cc/g)	BJH Average Pore Size (Å Diameter))	Ref.
Graphite	13.7	0.0270	22.4	[40]
GO	3.3	0.0095	31.3	[40]
rGO1	41.0	0.0513	22.5	[40]
rGO2	484.0	0.5050	22.2	(this study)

The thermal stabilities of the support materials were analyzed by TGA as shown in Fig. 3 (a). All measurements were carried out in air atmosphere up to 1000 ºC. In both support materials, the initial weight loss was observed between 250-500 °C and this loss can be attributed to the gasification of the carbonaceous material due to oxidation of rGO [40]. Above 500 ºC, almost a constant weight was observed up to 1000 ºC and both support materials showed very similar trend in weight loss by temperature. Also, the Pt loading amount of the catalysts were calculated from the weight percent loss difference between rGO supports and the Pt/rGO catalysts (Fig. 3 (b-c)). The calculated Pt loading (wt.%) values were given in Table 2 and it was observed that the Pt loading on rGO1 support was 25.2%, while the loading on rGO2 support was 20%.

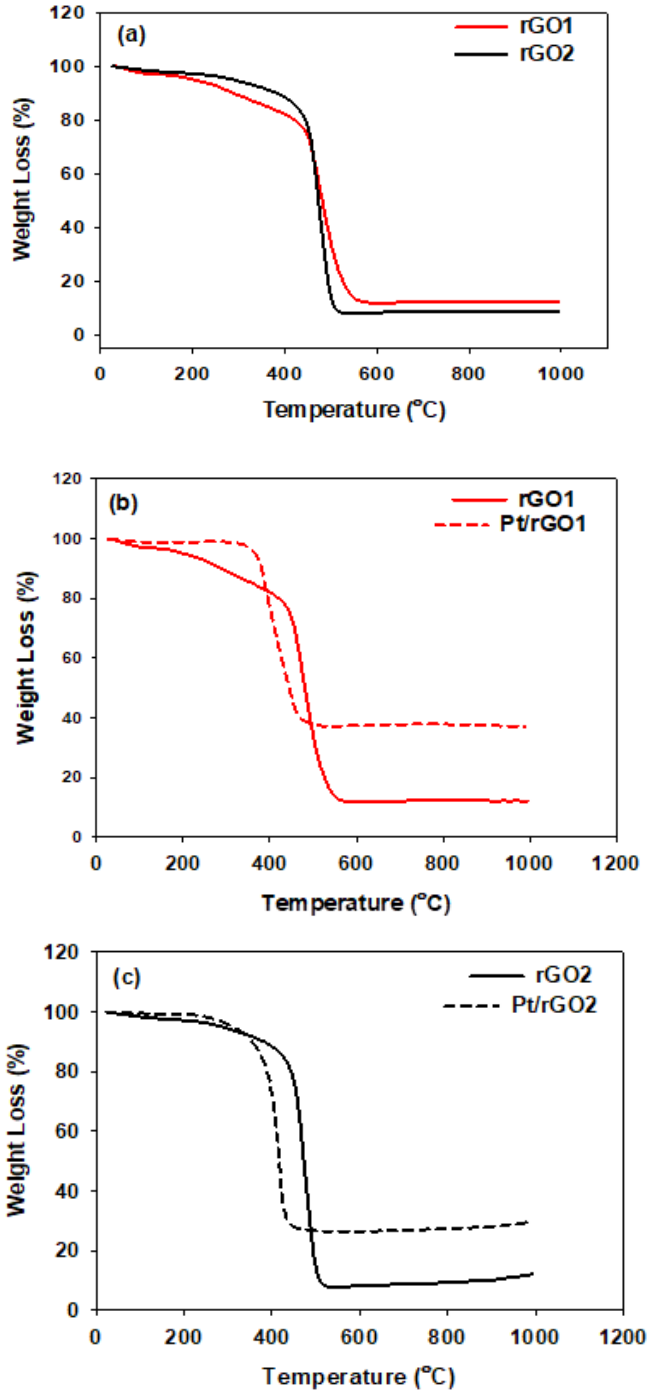

Figure 3. TGA curves of synthesized supports and catalysts

Table 2. Pt loading amounts of the catalysts

Catalyst	Pt [wt.%]
Pt/rGO1	25.2
Pt/rGO2	20

The morphology of the prepared support materials was investigated by using SEM. The obtained SEM plan-view images and corresponding EDS spectras were given in Fig. 4. The starting material was flake graphite having a flat morphology as shown in Fig. 4 (a). After the chemical oxidation process of graphite, the smooth flat structure turned into a rough and porous structure (Fig. 4 (b)). Also, the oxygen content increased owing to the formation of the oxygen functional groups on the edges and the basal planes of the rGO structure. In addition to the C and O atoms, the presence of new atoms such as S, K, Mn, Na were observed in the structure. Subsequently, the reduction process was carried out by using two different chemical reduction routes (as decribed in experimental part). Fig. 4 (c-d) shows the SEM images and corresponding EDS spectrums of the obtained rGO materials. As seen in the Fig. 4 (c), the rough surface structure of the GO changed into more uniform structure after reduction by DMF at reflux condition. Also, the purity of the material was checked by means of EDS and the spectra revealed that the structure still contain some residual impurities. In Fig. 4 (d) case, hydrazine hydrate was used to reduce GO. The obtained images showed that the structure contains micron-sized well-dispersed wrinkle flakes.

Fig. 5 displays TEM images of the rGO support materials and catalysts under different magnifications. In Fig. 5 (a) image, the rGO1 support material resembles a transparent ultrathin structure comprising few thin ripples within the plane, which is remarkably different from the opaque and smooth resemblance of pristine graphite flakes. This transparency and rippled characteristic of material, suggests that the material consists of a few thin layer or monolayer. Due to the wrinkled and overlapped structure, the individual graphene sheets can effectively link together and serve as great electrical conductor, resulting in high electrical conductivity [46]. On the other hand, the TEM image (Fig. 5 (b)) of rGO2 support material is composed of micrometer-sized wrinkled flakes with a high-transparency chiffon like texture. This wrinkle feature of the material prevents the aggregation of the dried sample due to van der Waals forces and play an important role in increasing the surface area [47].

Additionally, the TEM images of rGO supported Pt catalysts were also taken and results were given in Fig. 5 (c-d). It was clearly observed that the Pt NPs with spherical shaped particles were dispersed homogeneously on the rGO support materials. These results suggested that the $scCO_2$ deposition technique is a very accomplished method on the preparation of Pt NPs on rGO support materials.

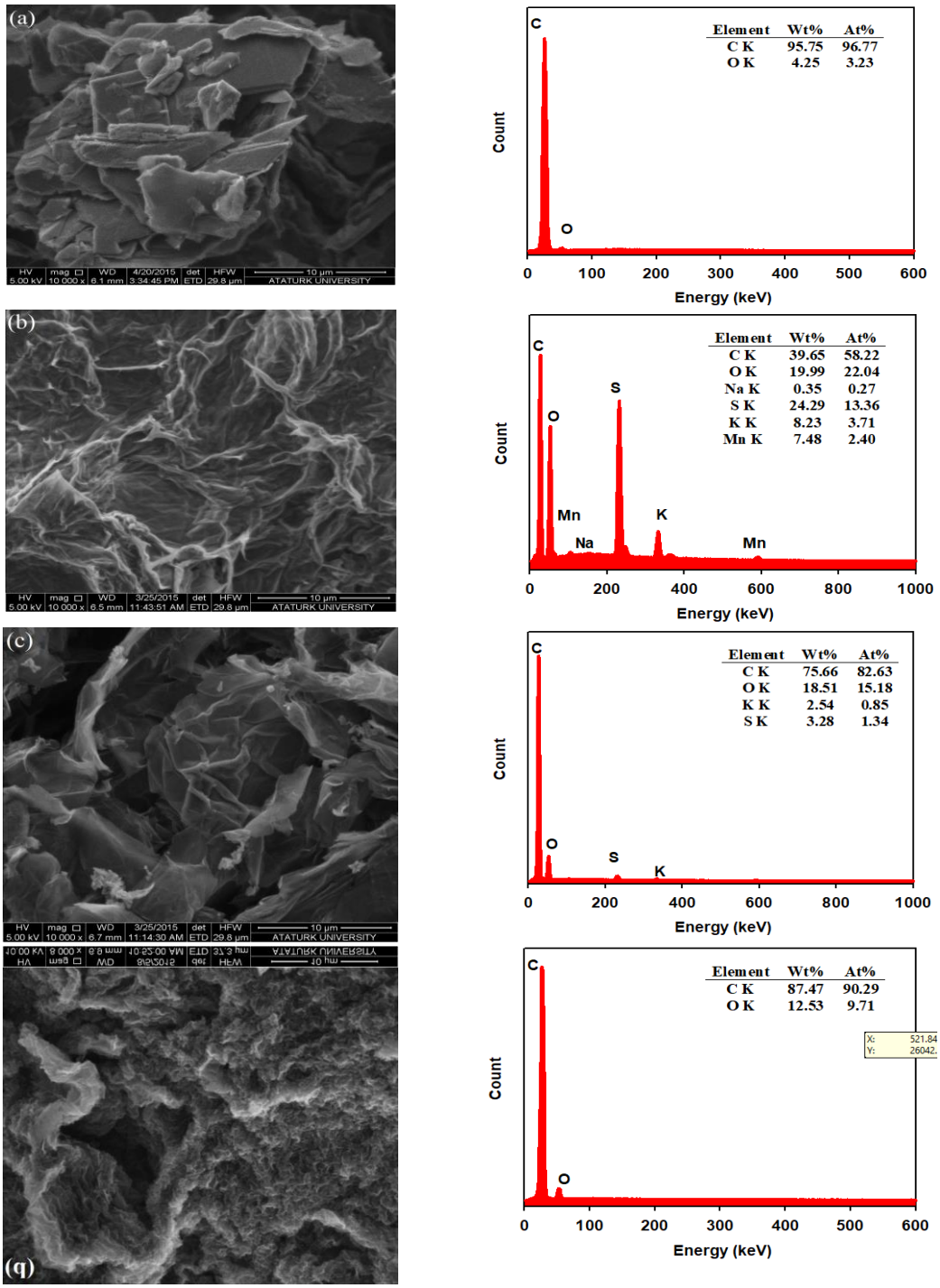

Figure 4. SEM and EDS results of (a) pristine graphite (b) GO (c) rGO1 (d) rGO2

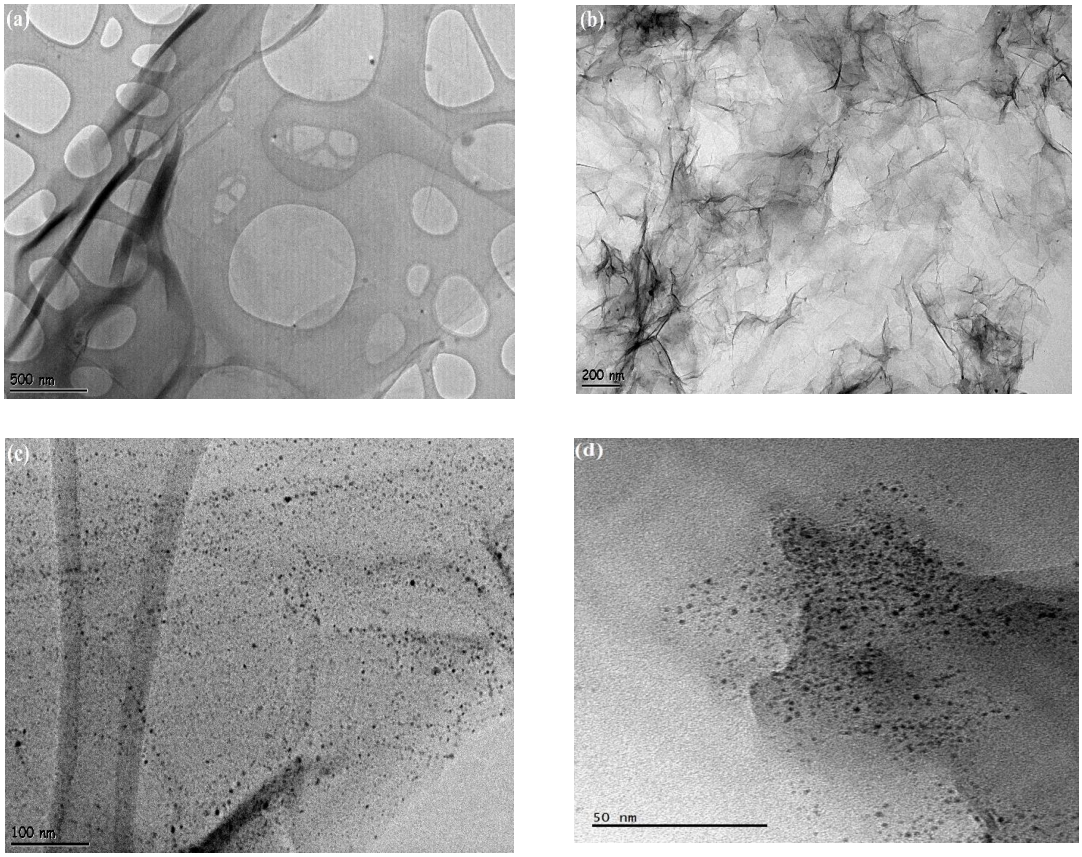

Figure 5. TEM images of (a) rGO1 (b) rGO2 (c) Pt/rGO1 (d) Pt/rGO2

Raman spectroscopy is an important characterization method used to evaluate the reduction effect and the main vibration peaks of carbon-based materials. Therefore, the pristine graphite and rGO support materials were characterized by Raman spectroscopy, as shown in Fig. 6. Two main characteristic peaks were observed for all the samples as D and G band. These bands are attributed to the defect/disorder states and the sp^2-bonded in plane vibration of carbon atoms, respectively [29, 48]. For the pristine graphite, the D and G band positions are centered at 1346 and 1572 cm^{-1} respectively, while for rGO1 and rGO2, these bands are centered at 1352 and 1593 and at 1352 and 1591 cm^{-1} respectively. The band positions and intensity ratios (I_D/I_G) of materials are summarized in Table 3.

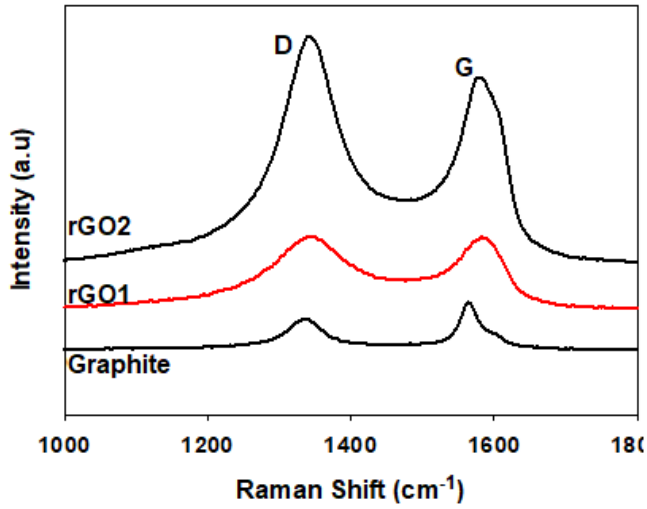

Figure 6. Raman spectra of pristine graphite, rGO1 and rGO2 support materials

Table 3. Analyses of Raman spectra

Sample	D band (cm^{-1})	G band (cm^{-1})	I_D/I_G
Graphite	1346	1572	0.48
rGO1	1352	1593	0.88
rGO2	1352	1591	1.22

As shown on Fig. 6 and Table 3, the Raman peaks showed change in band shape and band position. In the case of rGO, it is appears that the D band position of both rGO material is almost unchanged. However, the G band position of rGO's exhibit a shift toward higher wavenumber compare to the pristine graphite, which attributes to the restoration of the sp^2 bond of the carbon structure.

The intensity ratio (I_D/I_G) of these bands provides important information about the level of the disorder. The I_D/I_G ratio of graphite, rGO1 and rGO2 materials was found to be 0.48, 0.88 and 1.22 respectively. The high intensity ratio reveals that the defects increase after the reduced process. This increase of I_D/I_G upon GO reduction is normal and could be attributed to the generation of edge atoms in the structure and also residual oxygen containing groups, vacancies and topological defects from degraded functional groups.

On the other hand, a number of activity losses are observed in the catalyst and catalyst support materials under harsh operating conditions of PEM fuel cells. These losses are usually caused by reason such as fuel starvation, poor water management, CO poisoning in the anode electrode. If the fuel in the anode is insufficient, the voltage rises up to the value needed to oxidize the water to maintain the current. However, such a high potential leads to carbon corrosion and metal dissolution, causing the anode catalyst layer to degrade. Therefore, the use of corrosion-resistant materials is of great importance. For this purpose, the cyclic voltammetry measurements were carried out to examine the electrochemical oxidation (carbon corrosion) of rGO materials. The obtained voltammograms were shown in Fig. 7. The electrochemical oxidation tests were performed by applying 1.2 V in both support materials for 24 h. The voltammograms were performed in the range of -0.1 to 1.1 V against the normal hydrogen electrode (NHE). In both support

materials, faradaic peaks were observed at around 0.6 V of anodic scan and around 0.55 V of cathodic scan, corresponding to redox reactions of surface functionalities which provide pseudocapacitance. However, these anodic and cathodic peaks become more pronounced after the electrochemical oxidation. Furthermore, the peaks are shifted to higher and lower values after the electrochemical oxidation. Similar findings were observed for many carbon-based support materials which is reported in the literature [12, 49, 50] and ascribed to the dependence on the surface concentration of hydroquinone/quinone redox couple [51]. Also, it was seen that the CV currents have increased after reduction process for both support materials, which reflect surface area changes as well as the formation of new surface oxide groups, is correlated with the extent of carbon corrosion [50], although the exact relationship is not clear. According to the obtained CV results, it can be said that the rGO1 exhibits better electrochemical properties compared to rGO2 support.

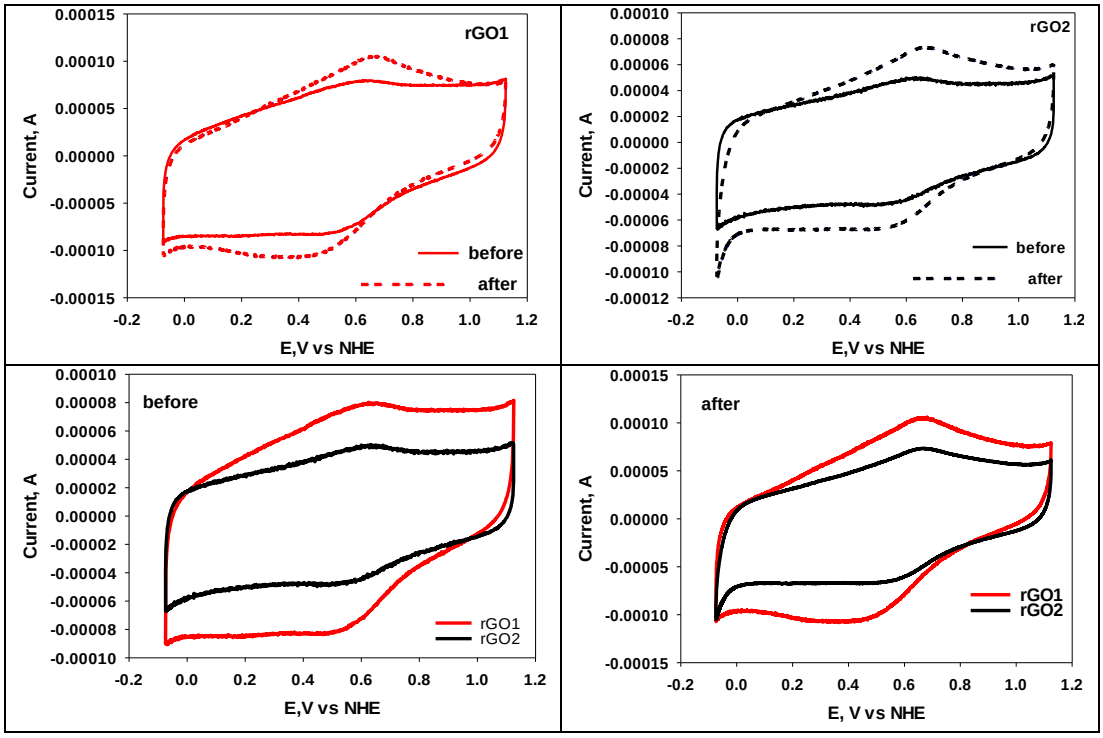

Figure 7. Cyclic voltammograms for rGO1 and rGO2 support materials before and after electrochemical oxidation

Fuel cell performances were also evaluated by using a single cell test station and the obtained polarization curves were given in Fig. 8. It was observed that the performance of the catalyst prepared with rGO1 support is higher than that of the rGO2 supported catalyst, especially at high current density region. This high fuel cell performance can be attributed to the structural properties of rGO1 support material, which provides superior mass transfer capability for reaction species compared to the rGO2 support material. The maximum power density achieved with the Pt/rGO1 catalyst is approximately 635 mW/cm^2 and higher than those reported maximum power density values for Pt/rGO (320 mW/cm^2) [52], Pt/rGO (375 mW/cm^2) [2], the partially GO-Pt (161 mW/cm^2) [25].

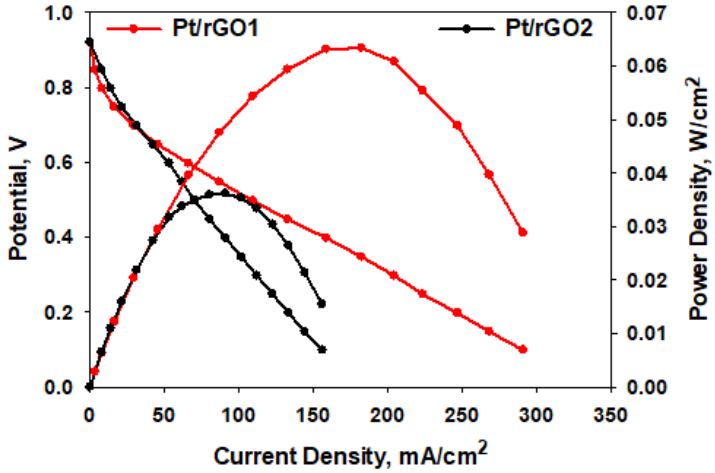

Figure 8. PEM fuel cell polarization curves

4. Conclusion

In summary, we have demostrated a facile and effective method for the preparation of rGO supported Pt NPs catalysts. Firstly, synthesis of rGO support materials were achieved by using two different reducing agents and then Pt NPs were created over these support materials by using $scCO_2$ deposition technique. To the best our knowledge, this is the first example of rGO supported Pt NPs where Pt NPs were decorated on the support by using $scCO_2$ deposition technique. The physicochemical and electrochemical experimental results showed that reducing agents used in the rGO support materials significantly affect the properties of the support materials and also PEM fuel cell performances. The maximum power density of 635 $mWcm^{-1}$ was achieved with Pt/rGO1 catalysts.

Acknowledgments
This work was supported by Atatürk University Scientific Research Project Council (Project No: 2014/79).

Conflicts of interest
The authors declare that there are no potential conflicts of interest relevant to this article.

References

[1] Acres G. J. K. Recent advances in fuel cell technology and its applications. Journal of Power Sources. 2001;100:60-66.

[2] Ozdemir OK. A novel method to produce few layers of graphene as support materials for platinum catalyst. Chemical Papers. 2018;73:387-95.

[3] Kou R, Shao Y, Wang D, Engelhard MH, Kwak JH, Wang J, et al. Enhanced activity and stability of Pt catalysts on functionalized graphene sheets for electrocatalytic oxygen reduction. Electrochemistry Communications. 2009;11:954-7.

[4] Daş E, Yurtcan AB. Effect of carbon ratio in the polypyrrole/carbon composite catalyst support on PEM fuel cell performance. International Journal of Hydrogen Energy. 2016;41:13171-9.

[5] Zhang M, Xie J, Sun Q, Yan Z, Chen M, Jing J. Enhanced electrocatalytic activity of high Pt-loadings on surface functionalized graphene nanosheets for methanol oxidation. International Journal of Hydrogen Energy. 2013;38:16402-9.

[6] Shao Y, Zhang S, Wang C, Nie Z, Liu J, Wang Y, et al. Highly durable graphene nanoplatelets supported Pt nanocatalysts for oxygen reduction. Journal of Power Sources. 2010;195:4600-5.

[7] Hellman H, Vandenhoed R. Characterising fuel cell technology: Challenges of the commercialisation process. International Journal of Hydrogen Energy. 2007;32:305-15.

[8] Bayrakçeken A, Smirnova A, Kitkamthorn U, Aindow M, Türker L, Eroğlu İ, et al. Pt-based electrocatalysts for polymer electrolyte membrane fuel cells prepared by supercritical deposition technique. Journal of Power Sources. 2008;179:532-40.

[9] Daş E, Bayrakçeken Yurtcan A. PEDOT/C Composites used as a Proton Exchange Membrane Fuel Cell Catalyst Support: Role of Carbon Amount. Energy Technology. 2017;5:1552-60.

[10] Dicks AL. The role of carbon in fuel cells. Journal of Power Sources. 2006;156:128-41.

[11] Oh H-S, Lee J-H, Kim H. Electrochemical carbon corrosion in high temperature proton exchange membrane fuel cells. International Journal of Hydrogen Energy. 2012;37:10844-9.

[12] Wang J, Yin G, Shao Y, Zhang S, Wang Z, Gao Y. Effect of carbon black support corrosion on the durability of Pt/C catalyst. Journal of Power Sources. 2007;171:331-9.

[13] Yu X, Ye S. Recent advances in activity and durability enhancement of Pt/C catalytic cathode in PEMFC. Journal of Power Sources. 2007;172:145-54.

[14] Liu B, Creager S. Carbon xerogels as Pt catalyst supports for polymer electrolyte membrane fuel-cell applications. Journal of Power Sources. 2010;195:1812-20.

[15] Cheng K, He D, Peng T, Lv H, Pan M, Mu S. Porous graphene supported Pt catalysts for proton exchange membrane fuel cells. Electrochimica Acta. 2014;132:356-63.

[16] Arbizzani C, Righi S, Soavi F, Mastragostino M. Graphene and carbon nanotube structures supported on mesoporous xerogel carbon as catalysts for oxygen reduction reaction in proton-exchange-membrane fuel cells. International Journal of Hydrogen Energy. 2011;36:5038-46.

[17] Sebastián D, Calderón JC, González-Expósito JA, Pastor E, Martínez-Huerta MV, Suelves I, et al. Influence of carbon nanofiber properties as electrocatalyst support on the electrochemical performance for PEM fuel cells. International Journal of Hydrogen Energy. 2010;35:9934-42.

[18] Trogadas P, Fuller TF, Strasser P. Carbon as catalyst and support for electrochemical energy conversion. Carbon. 2014;75:5-42.

[19] Sharma S, Pollet BG. Support materials for PEMFC and DMFC electrocatalysts—A review. Journal of Power Sources. 2012;208:96-119.

[20] Shao Y, Zhang S, Kou R, Wang X, Wang C, Dai S, et al. Noncovalently functionalized graphitic mesoporous carbon as a stable support of Pt nanoparticles for oxygen reduction. Journal of Power Sources. 2010;195:1805-11.

[21] Julkapli NM, Bagheri S. Graphene supported heterogeneous catalysts: An overview. International Journal of Hydrogen Energy. 2015;40:948-79.

[22] Soldano C, Mahmood A, Dujardin E. Production, properties and potential of graphene. Carbon. 2010;48:2127-50.
[23] Marinkas A, Arena F, Mitzel J, Prinz GM, Heinzel A, Peinecke V, et al. Graphene as catalyst support: The influences of carbon additives and catalyst preparation methods on the performance of PEM fuel cells. Carbon. 2013;58:139-50.
[24] Antolini E. Graphene as a new carbon support for low-temperature fuel cell catalysts. Applied Catalysis B: Environmental. 2012;123-124:52-68.
[25] Seger B, Kamat P. V. Electrocatalytically Active Graphene-Platinum Nanocomposites. Role of 2-D Carbon Support in PEM Fuel Cells. The Journal of Physical Chemistry C Letters.2009;113:7990-7995.
[26] Park S, Shao Y, Wan H, Rieke PC, Viswanathan VV, Towne SA, et al. Design of graphene sheets-supported Pt catalyst layer in PEM fuel cells. Electrochemistry Communications. 2011;13:258-61.
[27] Brownson DAC, Kampouris DK, Banks CE. An overview of graphene in energy production and storage applications. Journal of Power Sources. 2011;196:4873-85.
[28] Geng Y, Wang SJ, Kim JK. Preparation of graphite nanoplatelets and graphene sheets. J Colloid Interface Sci. 2009;336:592-8.
[29] Wang G, Yang J, Park J, Gou X, Wang B, Liu H, Yao J. Facile Synthesis and Characterization of Graphene Nanosheets. J. Phys. Chem. C. 2008;112:8192-8195.
[30] Stankovich S, Dikin DA, Piner RD, Kohlhaas KA, Kleinhammes A, Jia Y, et al. Synthesis of graphene-based nanosheets via chemical reduction of exfoliated graphite oxide. Carbon. 2007;45:1558-65.
[31] Dreyer DR, Park S, Bielawski CW, Ruoff RS. The chemistry of graphene oxide. Chem Soc Rev. 2010;39:228-40.
[32] Xin Y, Liu J-g, Zhou Y, Liu W, Gao J, Xie Y, et al. Preparation and characterization of Pt supported on graphene with enhanced electrocatalytic activity in fuel cell. Journal of Power Sources. 2011;196:1012-8.
[33] Daş E, Alkan Gürsel S, Işıkel Şanlı L, Bayrakçeken Yurtcan A. Thermodynamically controlled Pt deposition over graphene nanoplatelets: Effect of Pt loading on PEM fuel cell performance. International Journal of Hydrogen Energy. 2017;42:19246-56.
[34] Quesnel E, Roux F, Emieux F, Faucherand P, Kymakis E, Volonakis G, et al. Graphene-based technologies for energy applications, challenges and perspectives. 2D Materials. 2015;2.
[35] Zhang Y, Erkey C. Preparation of supported metallic nanoparticles using supercritical fluids: A review. The Journal of Supercritical Fluids. 2006;38:252-67.
[36] Bozbağ SE, Erkey C. Supercritical deposition: Current status and perspectives for the preparation of supported metal nanostructures. The Journal of Supercritical Fluids. 2015;96:298-312.
[37] Daş E, Kaplan BY, Gürsel SA, Yurtcan AB. Graphene nanoplatelets-carbon black hybrids as an efficient catalyst support for Pt nanoparticles for polymer electrolyte membrane fuel cells. Renewable Energy. 2019;139:1099-110.
[38] Bozbağ SE, Gümüşoğlu T, Yılmaztürk S, Ayala CJ, Aindow M, Deligöz H, et al. Electrochemical performance of fuel cell catalysts prepared by supercritical deposition: Effect of different precursor conversion routes. The Journal of Supercritical Fluids. 2015;97:154-64.
[39] N. I. Kovtyukhova, P. J. Ollivier, B. R. Martin, T. E. Mallouk, S. A. Chizhik, E. V. Buzaneva and A. D. Gorchinskiy, Layer-by-Layer Assembly of Ultrathin Composite Films from Micron-Sized Graphite Oxide Sheets and Polycations, Chem. Mater. 1999 (11) 771-778.
[40] Bayrakçeken Yurtcan A, Daş E. Chemically synthesized reduced graphene oxide-carbon black based hybrid catalysts for PEM fuel cells. International Journal of Hydrogen Energy. 2018;43:18691-701.

[41] Daş E, Alkan Gürsel S, Işikel Şanli L, Bayrakçeken Yurtcan A. Comparison of two different catalyst preparation methods for graphene nanoplatelets supported platinum catalysts. International Journal of Hydrogen Energy. 2016;41:9755-61.
[42] Bayrakçeken A, Cangül B, Zhang LC, Aindow M, Erkey C. PtPd/BP2000 electrocatalysts prepared by sequential supercritical carbon dioxide deposition. International Journal of Hydrogen Energy. 2010;35:11669-80.
[43] Brunauer S, Emmett P. H, Teller E. Adsorption of Gases in Multimolecular Layers. Journal of the American Chemical Society. 1938;60:309-319.
[44] Saquing CD, Cheng TT, Aindow M, Erkey C. Preparation of platinum/carbon aerogel nanocomposites using a supercritical deposition method. J. Phys. Chem. B. 2004;108:7716-22.
[45] Lebedeva NP, Janssen GJM. On the preparation and stability of bimetallic PtMo/C anodes for proton-exchange membrane fuel cells. Electrochemica Acta 2005;51:29-40.
[46] Mikhailov S. Physics and Applications of Graphene Experiments. ISBN: 978-953-307-217-3. Chapter 17, page 423.
[47] Yu S, Liu Q, Yang W, Han K, Wang Z, Zhu H. Graphene-CeO2 hybrid support for Pt nanoparticles as potential electrocatalyst for direct methanol fuel cells. Electrochim. Acta. 2013;94:245-251.
[48] Hasa B, Martino E, Vakros J, Trakakis G, Galiotis C, Katsaounis A. Effect of Carbon Support on the Electrocatalytic Properties of Pt–Ru Catalysts. ChemElectroChem. 2019;6:4970-9.
[49] Memioğlu F, Bayrakçeken A, Öznülüer T, Ak M. Synthesis and characterization of polypyrrole/carbon composite as a catalyst support for fuel cell applications. International Journal of Hydrogen Energy. 2012;37:16673-9.
[50] Schonvogel D, Hülstede J, Wagner P, Kruusenberg I, Tammeveski K, Dyck A, et al. Stability of Pt Nanoparticles on Alternative Carbon Supports for Oxygen Reduction Reaction. Journal of The Electrochemical Society. 2017;164:F995-F1004.
[51] Tarasevich M.R, Bogdanovskaya V. A, Zagudaeva N. M. Redox Reactions of Quinones on Carbon Materials. J. Electroanal. Chem. 1987;223:161-169.
[52] Şanlı LI, Bayram V, Yarar B, Ghobadi S, Gürsel SA. Development of graphene supported platinum nanoparticles for polymer electrolyte membrane fuel cells: Effect of support type and impregnation–reduction methods. International Journal of Hydrogen Energy. 2016;41:3414-27.